ISSN 2320-5407 International Journal of Advanced Research (2014), Volume 2, Issue 7, 1193-1207

ISSN NO. 2320-5407

Journal homepage: http://www.journalijar.com

INTERNATIONAL JOURNAL OF ADVANCED RESEARCH

RESEARCH ARTICLE

Lemon Essential Oil as Green Corrosion Inhibitor for α-brass in Nitric Acid Solutions

A.S. Fouda[1], A.M. Nofal[2], A. Awad[1], R. Riyad[1]

[1] Chemistry Department, Faculty of Science, Mansoura University, Mansoura-35516, Egypt

[2] Environmental Studies and Research Institute (ESRI), University of Sadat City, Egypt

Manuscript Info

Manuscript History:

Received: 12 May 2014
Final Accepted: 19 June 2014

Key words:

***Corresponding Author**

……………………

A. S. Fouda

Abstract

The effect of the addition of lemon oil on the corrosion of α-brass in nitric acid was investigated using weight loss, potentiodynamic polarization, electrochemical impedance spectroscopy (EIS) and electrochemical frequency modulation (EFM) measurements. It was found that lemon oil behaves as inhibitor. The inhibition efficiency increases with increasing the inhibitor concentration, but decreases with increasing the temperature. The adsorption of lemon oil on the α-brass surface follows Temkin's adsorption isotherm. The effect of the temperature in the range 298–313K on the corrosion of α-brass in 1M nitric acid was studied. Potentiodynamic polarization studies showed that this oil is mixed-type inhibitor and the results obtained from the different techniques were in good agreement.

Introduction

Copper and its alloys, because of their excellent resistance to corrosion in neutral aggressive media and their ease of processing, they are widely used in industries, particularly as condensers and heat exchangers in power plants (1). Electrochemical techniques are powerful tools to study brass since they offer valuable information about the phase and chemical composition (2). Such techniques have also proved to be useful to study the evolution of brass in the environment (3) to understand the degeneration process and to prevent oxidation of the alloy better (4-6). A number of studies have recently appeared in the literature (7-9) on the topic of the corrosion inhibition of α-brass in acidic medium. The aim of this paper is to describe an investigation of the inhibition of corrosion of commercial 57/43α-brass in 1 M HNO_3 solutions by some essential oils as lemon using weight-loss, potentiodynamic polarization measurements, electrochemical impedance spectroscopy (EIS) and electrochemical frequency modulation (EFM) measurements

Experimental technique

Materials

The experiments were performed with local commercial α-brass (Helwan Company of non-Ferrous Industries, Egypt) with the following composition (weight %) Cu 57, Zn 37, and some are additives. The inhibitor used was selected from essential oils.

Solutions

The aggressive solutions, 1 M HNO_3 were prepared by dilution of analytical grade (70 %) HNO_3 with bi-distilled water. All chemicals and reagents were of analytical grade. The measurements were performed in 1 M HNO_3 without and with the presence of lemon oil in the concentration range (1 to 5 ml\L).

.

Main constituents of Lemon oil are shown below:

The main chemical components of lemon oil are a-pinene, camphene, b-pinene, sabinene, myrcene, a-terpinene, linalool, β-bisabolene, limonene, trans-a-bergamotene, nerol and neral.

Weight loss tests

Six parallel α-brass sheets of 2 × 2 × 0.1 cm were abraded with emery paper (grade 400–600–800-1200) and then washed with bi-distilled water and acetone. After accurate weighing, the specimens were immersed in a 100 ml beaker, which contained 100 ml of HNO_3 with and without addition of different concentrations of lemon oil. All the aggressive acid solutions were open to air. After 3 h, the specimens were taken out, washed, dried, and weighed accurately. The average weight loss of the six parallel α-brass sheets could be obtained. The inhibition efficiency (% IE) and the degree of surface coverage, θ, of investigated oil for the corrosion of α-brass in HNO_3 were calculated from Eq. (1) (10):

$$\% IE = \theta \times 100 = [1-(W / W^\circ)] \times 100 \quad (1)$$

Where W° and W are the values of the average weight loss without and with addition of lemon oil, respectively.

Electrochemical Measurements

Potentiodynamic polarization measurements

Polarization experiments were carried out in a conventional three-electrode cell with platinum gauze as the auxiliary electrode and a saturated calomel electrode (SCE) coupled to a fine Luggin capillary as reference electrode. The working electrode was in the form of a square cut from copper sheet of equal composition embedded in epoxy resin of polytetrafluoroethylene so that the flat surface area was 1 cm^2. Prior to each measurement, the electrode surface was pretreated in the same manner as the weight loss experiments. Before measurements, the electrode was immersed in solution for 30 min. until a steady state was reached. The potential was started from -400 to + 400 mV vs. open circuit potential (E_{ocp}). All experiments were carried out in freshly prepared solutions at 25°C and results were always repeated at least three times to check the reproducibility. Then i_{corr} was used for the calculation of inhibition efficiency and surface coverage (θ) as below:

$$\%IE= \theta \times 100= (1-(i_{corr}/i^\circ_{corr}) \times 100 \quad (2)$$

Where i°_{corr} and i_{corr} are corrosion current densities in the absence and presence of lemon, respectively.

Electrochemical impedance spectroscopy (EIS) measurements

Impedance measurements were carried out using AC signals of 10 mV peak to peak amplitude at the open circuit potential in the frequency range of 100 kHz to 0.2 Hz. All impedance data were fitted to appropriate equivalent circuit using the Gamry Echem Analyst software version 6.03.

Electrochemical frequency modulation (EFM) measurements

EFM experiments were performed with applying potential perturbation signal with amplitude 10 mV with two sine waves of 2 and 5 Hz. The choice for the frequencies of 2 and 5 Hz was based on three arguments (11-13).The larger peaks were used to calculate the corrosion current density (i_{corr}), the Tafel slopes (β_c and β_a) and the causality factors CF-2 and CF-3(14).

The electrode potential was allowed to stabilize for 30 min before starting the measurements. All the experiments were conducted at 25 ± 1°C. Measurements were performed using Gamry Instrument Potentiostat/ Galvanostat/ ZRA (PCI4-G750). This includes a Gamry framework system v 6.03 Gamry applications include DC 105 software for DC corrosion measurements, EIS 300 software for electrochemical impedance spectroscopy measurements and EFM 140 for electrochemical frequency modulation measurements along with a computer for collecting data. Echem analyst v 6.03 software was used for plotting, graphing, and fitting data.

Surface examination

The surface films were formed on the α-brass specimens by immersing them in inhibitor solutions for a period of 24 h. After the immersion period, the specimens were taken out, dried and the nature of the film formed on the surface of the metal specimen was analyzed by SEM technique. Examination of α-Brass surface after 24 h exposure to the 1 M HNO_3 solution without and with inhibitor was carried out by JOEL JSM-6510LVScanning Electron Microscope.

Results and Discussion

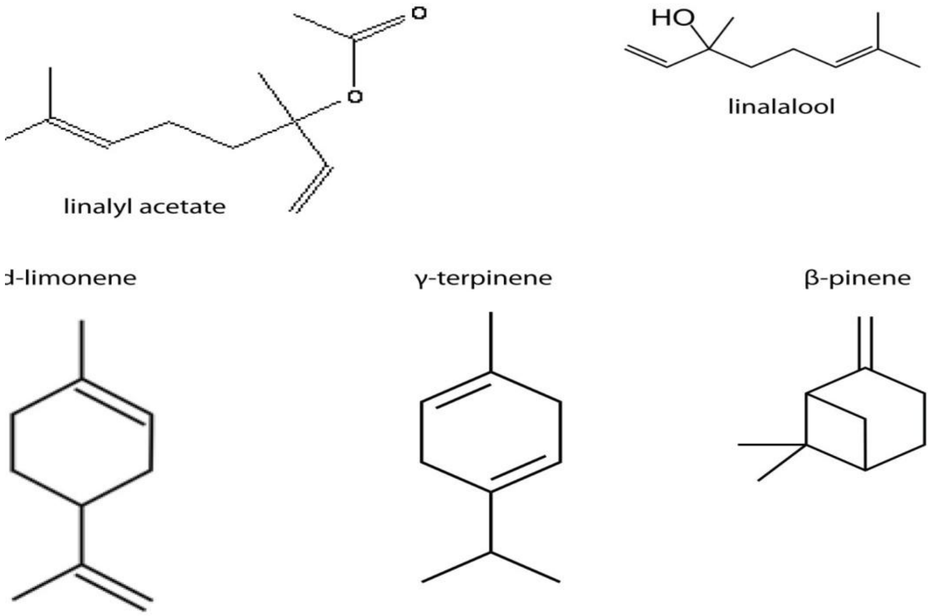

Figure 1 Structure of linalyl acetate. Linalool d-limonene, γ-terpine and β -pinene

Weight-Loss Measurements

Weight-loss of α-brass was determined, at various time intervals, in the absence and presence of different concentrations of the inhibitor. The obtained weight-loss time curves are represented in Figure 2 for Lemon. The inhibition efficiency of corrosion was found to be dependent on the inhibitor concentration. The curves obtained in the presence of inhibitor fall significantly below that of free acid. In all cases, the increase in the inhibitor concentration was accompanied by a decrease in weight-loss and an increase in the percentage inhibition. These results lead to the conclusion that lemon oil under investigation is fairly efficient as inhibitor for α-brass dissolution in nitric acid solution. Also, the degree of surface coverage (Θ) by the inhibitor, calculated from Eq. (1), would increase by increasing the inhibitor concentration.

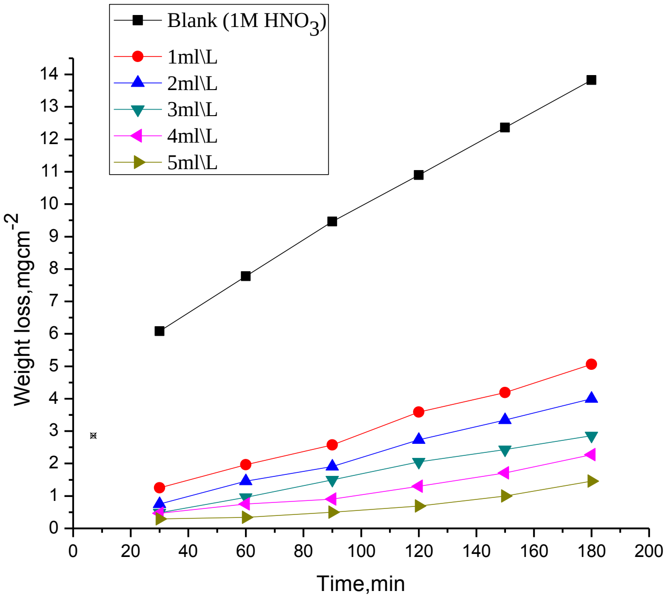

Figure 2: Weight loss-time curves for the corrosion of α-brass in 1 M HNO_3 in the absence and presence of different concentrations of lemon oil at 298K

Table 1: Values of inhibition efficiencies (%IE) and surface coverage (θ) of inhibitor for the corrosion of α-brass in 1 M HNO_3 from weight-loss measurements at different concentrations and at 298 K

[inh] Ml\L	Lemon	
	Θ	% IE
1	0.6709	67.09
2	0.7497	74.97
3	0.8119	81.19
4	0.8806	88.06
5	0.9365	93.65

Effect of Temperature

The effect of temperature on the corrosion rate of α-brass in 1M HNO_3 and in presence of different inhibitor concentrations was studied in the temperature range of 298–313K using weight loss measurements .As the temperature increases, the rate of corrosion increases and the inhibition efficiency of the additives decreases as shown in Table2 for Lemon. The adsorption behavior of inhibitor on α- brass surface occurs through physical adsorption.

Table 2: Values of inhibition efficiencies %IE and corrosion rate (C.R) of Lemon for the corrosion of α-brass in 1 M HNO_3 from weight-loss measurements at different concentrations at temperature range of 298-313 K

[inh] Ml\L	298 K		303K		308K		313K	
	C.R	% IE	C.R	%IE	C.R	%IE	C.R	%IE
1	0.030	67.09	0.032	58.41	0.034	46.07	0.12	44.55
2	0.023	74.97	0.025	71.33	0.026	60.77	0.09	59.22
3	0.017	81.19	0.020	79.81	0.021	72.37	0.06	71.04
4	0.011	88.06	0.017	85.87	0.019	79.19	0.05	74.53
5	0.006	93.64	0.013	93.54	0.015	88.34	0.04	79.69

Adsorption Isotherm

One of the most convenient ways of expressing adsorption quantitatively is by deriving the adsorption isotherm that characterizes the metal/inhibitor/ environment system. Various adsorption isotherms were applied to fit θ values, but the best fit was found to obey Temkin adsorption isotherm which are represented in Figure 3 for Lemon, Temkin adsorption isotherm may be expressed by:

$$a\Theta = \ln K C \qquad (3)$$

Where C is the concentration (ml\L) of the inhibitor in the bulk electrolyte, is the degree of surface coverage (Θ=% IE/100), K_{ads} is the adsorption equilibrium constant. A plot of Θ versus log C should give straight lines with slope equal 2.303/a and the intercept is (2.303/a log K). The variation of the adsorption equilibrium constant (K_{ads}) of the inhibitor with their molar concentrations was calculated according to Eq. (2). The experimental data give good curves fitting for the applied adsorption isotherm as the correlation coefficients (R^2) were in the range (0.943-0.999). The values obtained are given in Table 3.

The equilibrium constant of adsorption K_{ads} obtained from the intercepts of Temkin adsorption isotherm is related to the free energy of adsorption ΔG° ads as follows:

$K_{ads}=1/55.5 \exp [-\Delta G° ads] / RT]$ (4)

Where, 55.5 is the molar concentration of water in the solution in M^{-1}

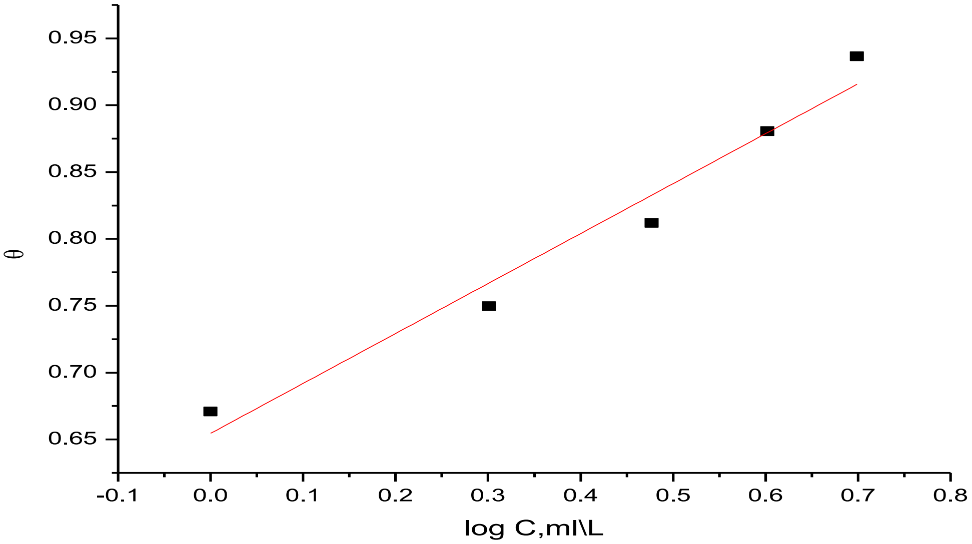

Figure 3: Temkin adsorption isotherm of lemon oil on α-brass surface in 1 M HNO_3 at 298K

Table 3.Equilibrium constant (K_{ads}) of lemon oil adsorbed on α-brass surface in 1M HNO_3 at 298K

Temp °C	Lemon	
	K_{ads} x10^{-3} M^{-1}	α
25	3.72	6.16
30	7.08	4.71
35	13.46	4.54
40	21.18	3.88

Plot of (ΔG^o_{ads}) versus T Figure 4 gave the heat of adsorption (ΔH^o_{ads}) and the standard entropy (ΔS^o_{ads}) according to the thermodynamic basic equation 3:

$\Delta G^o_{ads} = \Delta H^o_{ads} - T\ \Delta s^o_{ads}$

Table 4 clearly shows a good dependence of ΔG^o_{ads} on T, indicating the good correlation among thermodynamic parameters. The negative value of ΔG^o_{ads} ensures the spontaneity of the adsorption process and stability of the adsorbed layer on α- brass surface. Generally, values of ΔG^o_{ads} around -20 kJ mol^{-1} or lower are consistent with the electrostatic interaction between the charged molecules and the charged metal (physical adsorption).The calculated ΔG^o_{ads} values are closer to -20 kJ mol^{-1} indicating that the adsorption mechanism of the inhibitor on α-brass in 1 M HNO_3 solutions was typical of physical adsorption. The values of thermodynamic parameter for the adsorption of inhibitor Table 4 can provide valuable information about the mechanism of corrosion inhibition. While an endothermic adsorption process ($\Delta H^o_{ads} > 0$) is attributed unequivocally to an exothermic adsorption process

($\Delta H^o_{ads}<0$) may involve either exothermic adsorption or endothermic adsorption or mixture of both processes. In the presented case, the calculated values of $\Delta H^\circ_{ads}$for the adsorption of inhibitor in 1 M HNO_3 indicating that lemon oil may be physically adsorbed. The ΔS^o_{ads} values in the presence of inhibitor in 1 M HNO_3 are positive. . This indicates that an increase in disorder takes places on going from reactants to the metal-adsorbed reaction complex (15).

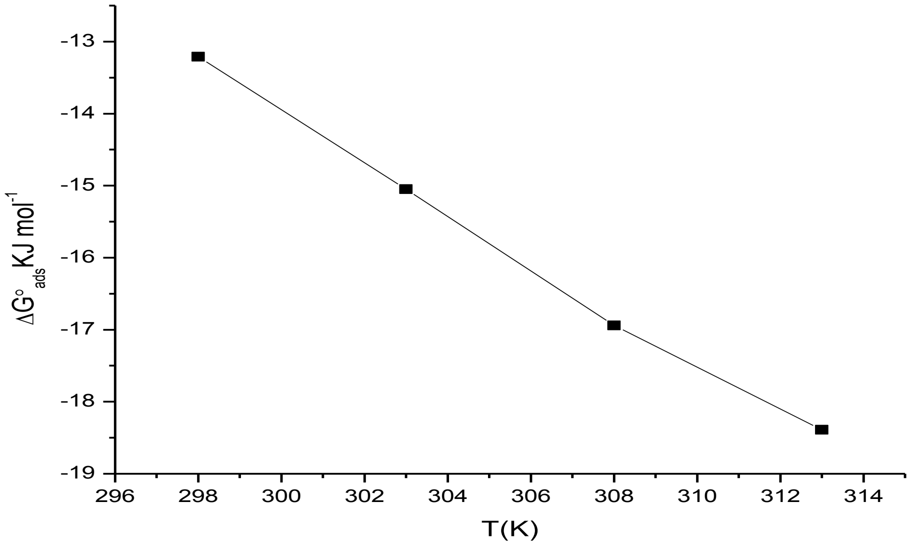

Figure 4: Variation of ΔG^o_{ads} versus T for the adsorption of inhibitor on α-brass surface in 1 M HNO_3 at different temperature

Table 4: Thermodynamic parameters for the adsorption of lemon oil on α-brass surface in 1 M HNO_3 at different temperatures

Inhibitor	Temperature °C	K_{ads} M^{-1}	$-\Delta G^o_{ads}$ kJ mol^{-1}	ΔH^o_{ads} kJ mol^{-1}	ΔS^o_{ads} J $mol^{-1}K^{-1}$
Lemon	25	3.72	13.2081	90.86085	349.225
	30	7.08	15.0512		349.545
	35	13.46	16.94499		350.019
	40	21.12	18.39261		349.053

Kinetic –Thermodynamic Corrosion Parameters

The activation parameters for the corrosion process were calculated from Arrhenius-type plot according to eq. (6):

$k_{corr=}$A exp (E^*_a/RT) (6)

Where E^*_a is the apparent activation corrosion energy, R is the universal gas constant, T is the absolute temperature and A is the Arrhenius pre-exponential constant. Values of apparent activation energy of corrosion for α-brass in 1 M HNO_3 shown in Table 5, without and with various concentrations of lemon oil determined from the slope of log (k_{corr}) versus 1/T plots are shown in Figure 5. Inspection of the data shows that the activation energy is lower in the presence of inhibitor than in its absence. This was attributed to slow rate of inhibitor adsorption with a resultant closer approach to equilibrium during the experiments at higher temperatures according to Hoar and Holliday (16). But, Riggs and Hurd (17) explained that the decrease in the activation energy of corrosion at higher levels of inhibition arises from a shift of the net corrosion reaction from the uncovered part of the metal surface to the covered one. Schmid and Huang (18) found that organic molecules inhibit both the anodic and cathodic partial reactions on the electrode surface and a parallel reaction takes place on the covered area, but the reaction rate on the covered area is substantially less than on the uncovered area similar to the present study. The alternative formulation of transition state equation is shown in Eq. (7):

k_{corr} = (RT/Nh) exp (ΔS^*/R)exp ($-\Delta H^*$/RT) (7)

Where $k_{corr}$is the rate of metal dissolution, h is Planck's constant, N is Avogadro's number, ΔS^* is the entropy of activation and ΔH^* is the enthalpy of activation.

Figure 5 shows a plot of log k against (1/T) in 1 M HNO_3. Straight lines are obtained with a slopes equal to (ΔH^* /2.303R) and intercepts are [log (R/Nh + ΔS^*/2.303R)] are calculated Table 5.
The increase in E_a^* with increase inhibitor concentration Table 5 is typical of physical adsorption. The positive signs of the enthalpies (ΔH^*) reflect the endothermic nature of the α-brass dissolution process. Value of entropies (ΔS^*) imply that the activated complex at the rate determining step represents an association rather than a dissociation step, meaning that a decrease in disordering takes place on going from reactants to the activated complex (19,20).

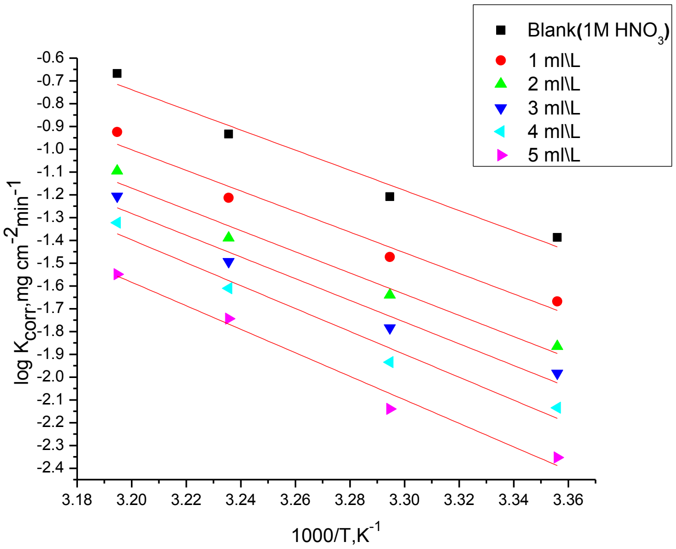

Figure 5: Log k vs. (1/T) curves for Arrhenius plots for α-brass corrosion rates (k_{corr}) after 120 minute of immersion in 1M HNO_3 in the absence and presence of various concentrations of lemon oil

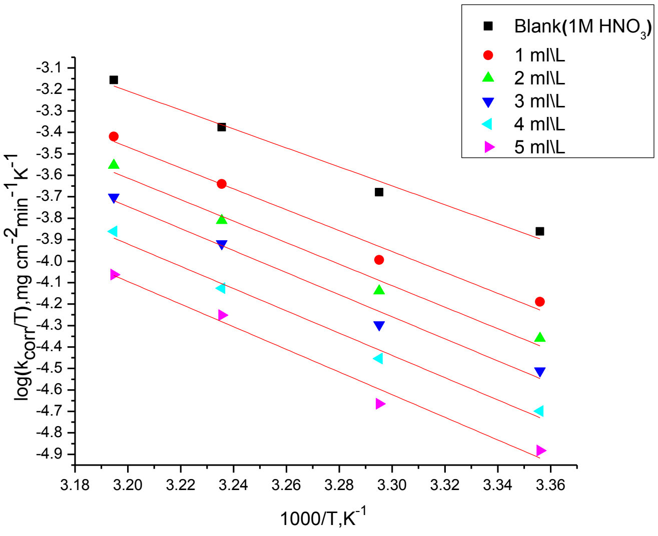

Figure 6: Log (k/T) vs. (1/T) curves for Transition plots for α-brass corrosion rates (k_{corr}) after 120 minute of immersion in 1M HNO_3 in the absence and presence of various concentrations of lemon oil

Table 5: Activation parameters for α-brass corrosion in the absence and presence of various concentrations of lemon oil in 1M HNO_3

Inhibitor	**[inh] Ml\L**	**E_a^* kJ mol^{-1}**	**ΔH* kJ mol^{-1}**	**ΔS* J mol^{-1}K^{-1}**	**A x10^7 g cm^{-2} min^{-1}**
Blank	0	84.20	36.52	10.12	1.703
Lemon	1	87.20	40.20	32.18	2.860
	2	88.91	41.48	38.90	5.269
	3	92.18	42.38	43.00	9.174
	4	96.25	42.92	43.60	47.980
	5	98.78	43.87	47.19	84.410

Potentiodynamic Polarization Measurements

Figures 7 show typical polarization curves for α-brass in 1 M HNO_3 media. The two distinct regions that appeared were the active dissolution region (apparent Tafel region), and the limiting current region. In the inhibitor-free solution, the anodic polarization curve of copper showed a monotonic increase of current with potential until the current reached the maximum value. After this maximum current density value, the current density declined rapidly with potential increase, forming an anodic current peak that was related to Cu $(NO_3)_2$ film formation. In the presence of inhibitor, both the cathodic and anodic current densities were greatly decreased over a wide potential range. Various corrosion parameters such as corrosion potential ($E_{corr.}$), anodic and cathodic Tafel slopes ($β_a$, $β_c$), the corrosion current density (i_{corr}), the degree of surface coverage (θ) and the inhibition efficiency (%IE) are given in Table6. It can see from the experimental results that in all cases, addition of inhibitor induced a significant decrease in cathode and anodic currents. The values of E_{corr} were affected and slightly changed by the addition of inhibitor. This indicates that lemon oil acts as mixed-type inhibitor. The slopes of anodic and cathodic Tafel lines ($β_a$ and $β_c$), were slightly changed (Tafel lines are parallel), on increasing the concentration of lemon oil which indicates that there is no change of the mechanism of inhibition in the presence and absence of inhibitor. The orders of inhibition efficiency of inhibitor at different concentrations as given by polarization measurements are listed in Table 6. The results are in good agreement with those obtained from weight-loss measurements.

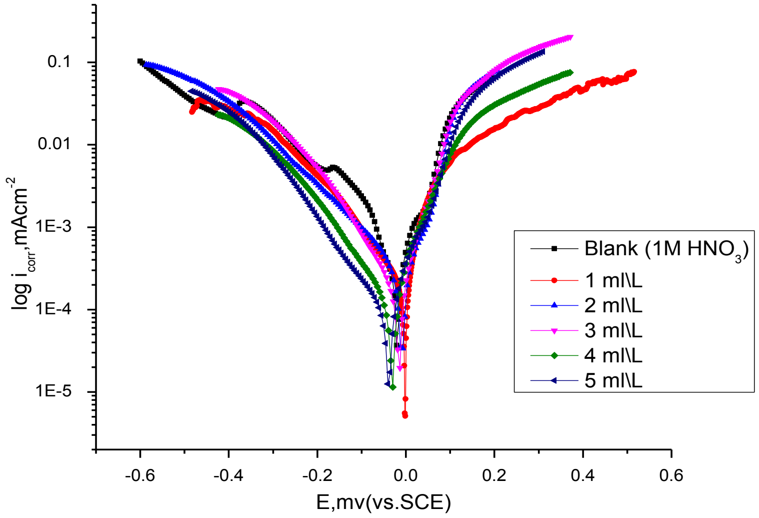

Figure 7: Potentiodynamic polarization curves for the dissolution of α-brass in 1M HNO_3 in the absence and presence of different concentrations of the lemon oil at 298K

Table 6: Corrosion potential (E_{corr}), corrosion current density (i_{corr}), Tafel slopes (β_c, β_a), degree of surface coverage (θ), and inhibition efficiency (% IE) of α-brass in 1M HNO_3 at 298 K for lemon oil

Inhibitor	[inh] $x10^6$ M	$-E_{corr}$ mV vs SCE	i_{corr} $\mu A\ cm^{-2}$	β_a $mV\ dec^{-1}$	β_c $mV\ dec^{-1}$	Θ	% IE
Blank	0	19.20	791	124	205	----	----
Lemon	1	1.83	376	112.7	191.9	0.525	52.5
	2	9.60	309	74.90	190.4	0.609	60.9
	3	15.30	225	63.9	146.2	0.716	71.6
	4	30.90	167	80.20	160	0.789	78.9
	5	38.50	100	72.8	142.4	0.874	87.4

Electrochemical Impedance Spectroscopy (EIS) Measurements

EIS is well-established and it is powerful technique for studying the corrosion. Surface properties, electrode kinetics and mechanistic information can be obtained from impedance diagrams (21-25).Figure9 shows the Nyquist (a) and Bode (b) plots obtained at open-circuit potential both in the absence and presence of increasing concentrations of lemon oil at 25°C. The increase in the size of the capacitive loop with the addition of lemon oil shows that a barrier gradually forms on the α-brass surface. The increase in the capacitive loop size (Figure 9a) enhances, at a fixed inhibitor concentration, following the order. Bode plots (Figure 9b), shows that the total impedance increases with increasing inhibitor concentration (log Z vs. log f). But (log f vs. phase), also Bode plot shows the continuous increase in the phase angle shift, obviously correlating with the increase of inhibitor adsorbed on α-brass surface. The Nyquist plots do not yield perfect semicircles as expected from the theory of EIS. The deviation from ideal semicircle was generally attributed to the frequency dispersion (26) as well as to the inhomogenities of the surface.

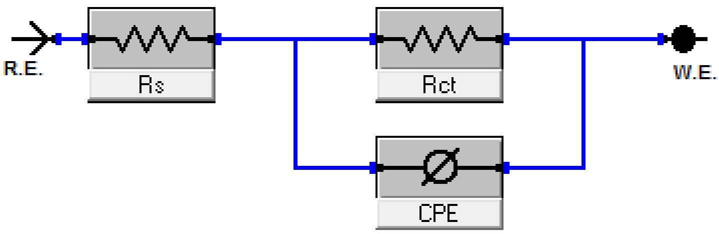

Figure 8: Equivalent circuit model used to fit experimental EIS

EIS spectra of the investigated compound were analyzed using the equivalent circuit, Figure 8, which represents a single charge transfer reaction and fits well with our experimental results. The constant phase element, CPE, is introduced in the circuit instead of a pure double layer capacitor to give a more accurate fit (27).The double layer capacitance, C_{dl}, for a circuit including a CPE parameter (Y_0 and n) were calculated from eq.8 (28) :

$$C_{dl} = Y_0 (\omega_{max})^{n-1} \qquad (8)$$

whereY_0 is the magnitude of the CPE, $\omega_{max} = 2\pi f_{max}$, f_{max} is the frequency at which the imaginary component of the impedance is maximal and the factor n is an adjustable parameter that usually lies between 0.50 and 1.0. After analyzing the shape of the Nyquist plots, it is concluded that the curves approximated by a single capacitive semicircles, showing that the corrosion process was mainly charged-transfer controlled (29,30) .The general shape of the curves is very similar for all samples (in presence or absence of inhibitor at different immersion times) indicating that no change in the corrosion mechanism (31).From the impedance data Table 7, we concluded that the value of R_{ct} increases with increasing the concentration of the inhibitor and this indicates an increase in % IE_{EIS}, which in concord with the EFM results obtained. In fact the presence of inhibitors enhances the value of R_{ct} in acidic solution. Values of double layer capacitance are also brought down to the maximum extent in the presence of inhibitor and the decrease in the values of CPE follows the order similar to that obtained for i_{corr} in this study. The decrease in CPE/C_{dl} results from a decrease in local dielectric constant and/or an increase in the thickness of the double layer, suggesting that organic derivatives inhibit the copper corrosion by adsorption at metal/acid (32, 33) .The inhibition efficiency was calculated from the charge transfer resistance data from eq.9 (34):

$$\% IE_{EIS} = [1 - (R^{\circ}ct / R_{ct})] \times 100 \quad (9)$$

Where R^{o}_{ct} and Rct are the charge-transfer resistance values without and with inhibitor respectively.

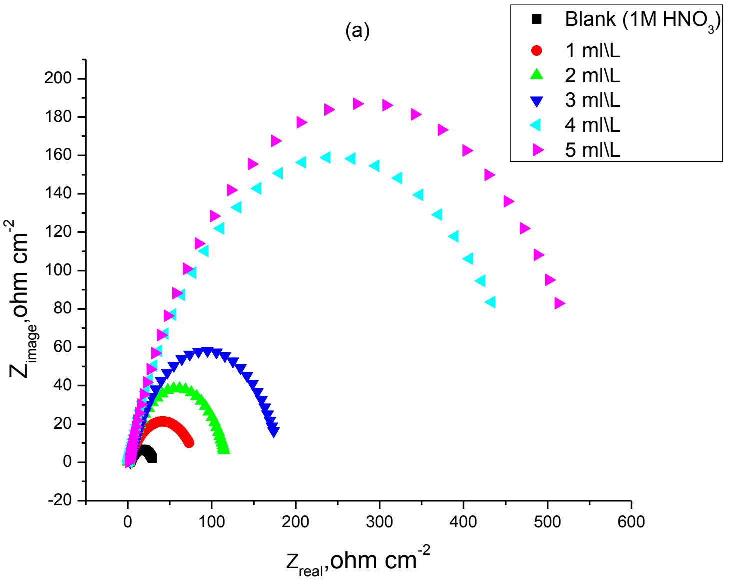

Figure 9a: The Nyquist plots for the corrosion of α-brass in 1M HNO_3 in the absence and presence of different concentrations of lemon oil at **298K**

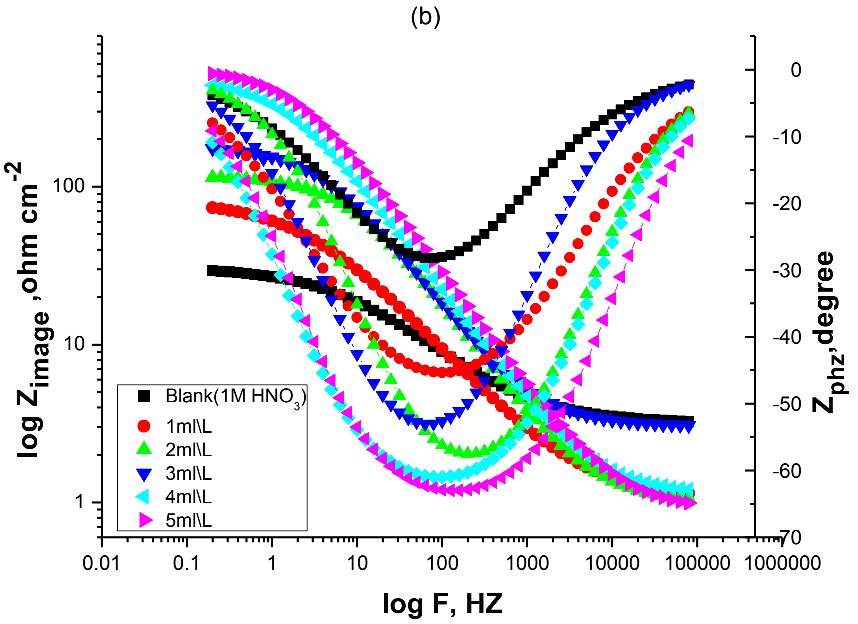

Figure 9 b: The Bode plots for the corrosion of α-brass in 1M HNO_3 in the absence and presence of different concentrations of lemon oil at 298K

Table 7: Electrochemical kinetic parameters obtained by EIS technique for α-brass in 1 M HNO3 without and with various concentrations of lemon oil at **298K**

Inhibitor	[inh] x10^6 M	R_{ct} Ω cm^2	R_s Ω cm^2	C_{dl} μFcm^{-2}	Θ	% IE
Blank	0	27.96	3.153	546	-----	------
Lemon	1	81.43	1.046	267	0.657	65.7
	2	116.8	1.002	260	0.761	76.1
	3	179.9	3.021	213	0.845	84.5
	4	490.0	1.127	210	0.943	94.3
	5	563.6	0.898	151	0.950	95.0

Electrochemical Frequency Modulation (EFM) Measurements

EFM is a nondestructive corrosion measurement technique that can directly and quickly determine the corrosion current values without prior knowledge of Tafel slopes, and with only a small polarizing signal. These advantages of EFM technique make it an ideal candidate for online corrosion monitoring (35).The great strength of the EFM is the causality factors which serve as an internal check on the validity of EFM measurement. The causality factors CF-2 and CF-3 are calculated from the frequency spectrum of the current responses.

Figure 10 shows the EFM Intermodulation spectra (current vs frequency) of α-brass in HNO_3 solution containing different concentrations of lemon oil. The harmonic and intermodulation peaks are clearly visible and are much larger than the background noise. The two large peaks, with amplitude of about 200 µA, are the response to the 40 and 100 mHz (2 and 5 Hz) excitation frequencies. It is important to note that between the peaks there is nearly no current response (<100 nA). The experimental EFM data were treated using two different models: complete diffusion control of the cathodic reaction and the "activation" model. For the latter, a set of three non-linear equations had been solved, assuming that the corrosion potential does not change due to the polarization of the working electrode (36).The larger peaks were used to calculate the corrosion current density (i_{corr}), the Tafel slopes (β_c and β_a) and the causality factors (CF-2 and CF-3).These electrochemical parameters were listed in Table 8.The data presented in Table 8 obviously show that, the addition of lemon oil at a given concentration to the acidic solution decreases the corrosion current density, indicating that this compound inhibits the corrosion of α-brass in 1 M HNO_3 through adsorption. The causality factors obtained under different experimental conditions are approximately equal to the theoretical values (2 and 3) indicating that the measured data are verified and of good quality. The inhibition efficiencies $\%IE_{EFM}$ increase by increasing the inhibitor concentrations and was calculated as from Eq. (10):

$$\%IE_{EFM} = [1-(i_{corr}/i^{o}_{corr})] \times 100 \qquad (10)$$

Where i^{o}_{corr} and i_{corr} are corrosion current densities in the absence and presence of lemon oil

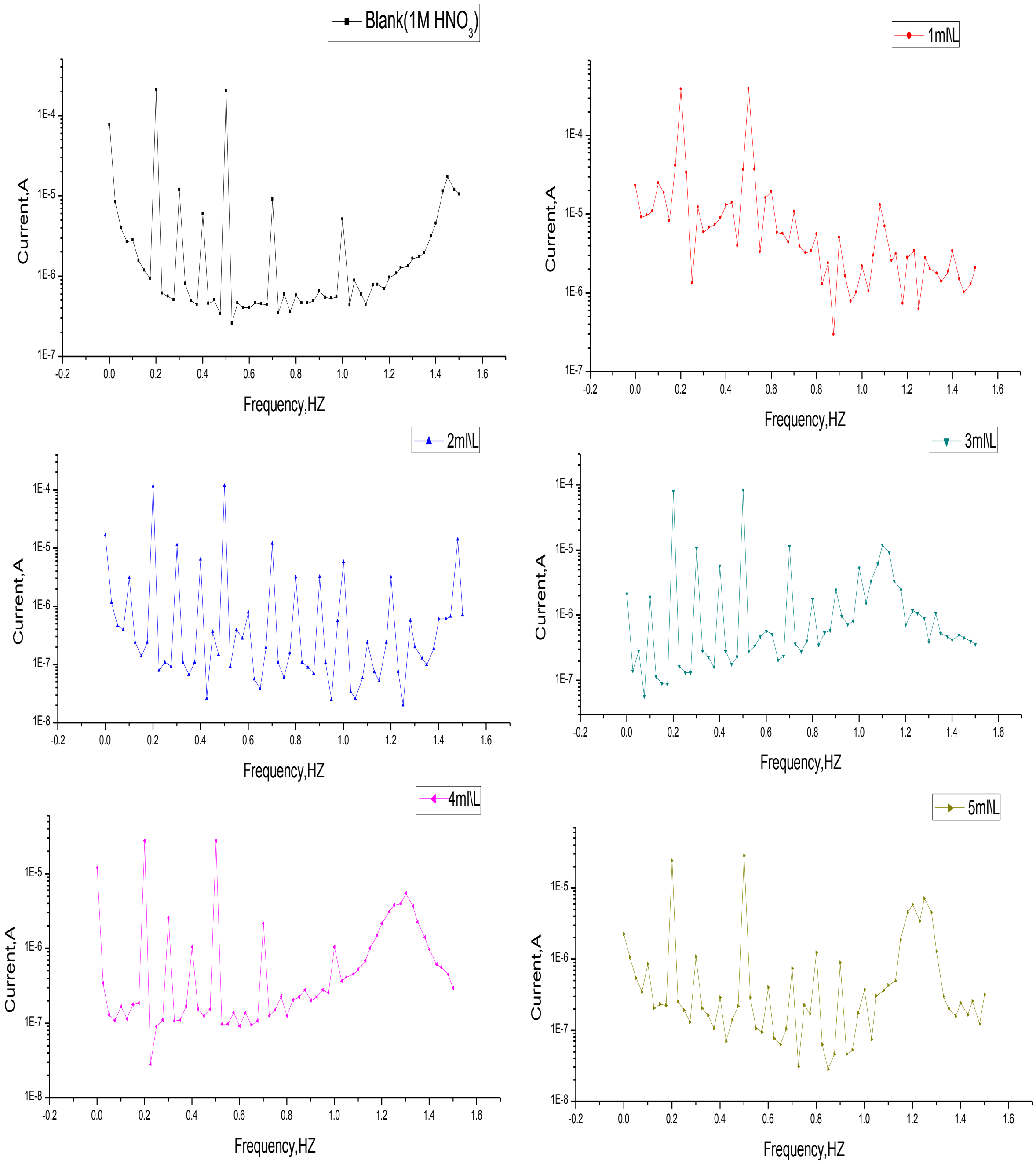

Figure 10: EFM spectra for α-brass in 1 M HNO_3 in the absence and presence of different concentrations of Lemon oil at 298K

Table 8: Electrochemical kinetic parameters obtained from EFM technique for α-brass in 1M HNO_3 in the absence and presence of different concentrations of lemon oil

Inh	[inh]x10^6 M	i_{corr} μAcm^{-2}	β_a $mVdec^{-1}$	β_c $mVdec^{-1}$	CF-2	CF-3	C.R mpy	Θ	% IE
Blank	0	501.5	128	215	1.897	2.304	223	-	-
Lemon	1	442.3	70	77	1.100	0.899	196.7	0.485	48.5
	2	136.2	61	98	1.897	4.240	60.55	0.706	70.6
	3	122.7	69	159	1.954	3.705	54.58	0.711	71.1
	4	33.88	65	100	2.256	3.457	15.07	0.712	71.2
	5	16.38	38	42	2.758	6.142	7.29	0.717	71.7

SEM examination

In order to verify if the lemon oil molecules are in fact adsorbed on α-brass surface, SEM experiments were carried out. The SEM micrographs for α-brass surface alone and after 24 h immersion in 1 M HNO3 without and with the addition of 5 ml\L of lemon oil are shown in Figures (11a-c). As expected, Figure11ashows metallic surface is clear, while in the absence of lemon oil, the α-brass surface is damaged by HNO_3 corrosion (Figure11b). In contrast, in presence of the investigated compound (Figures (11c)); the metallic surface seems to be almost no affected by corrosion. The formation of a thin film of lemon oil observed in SEM micrograph, thus protecting the surface against corrosion.

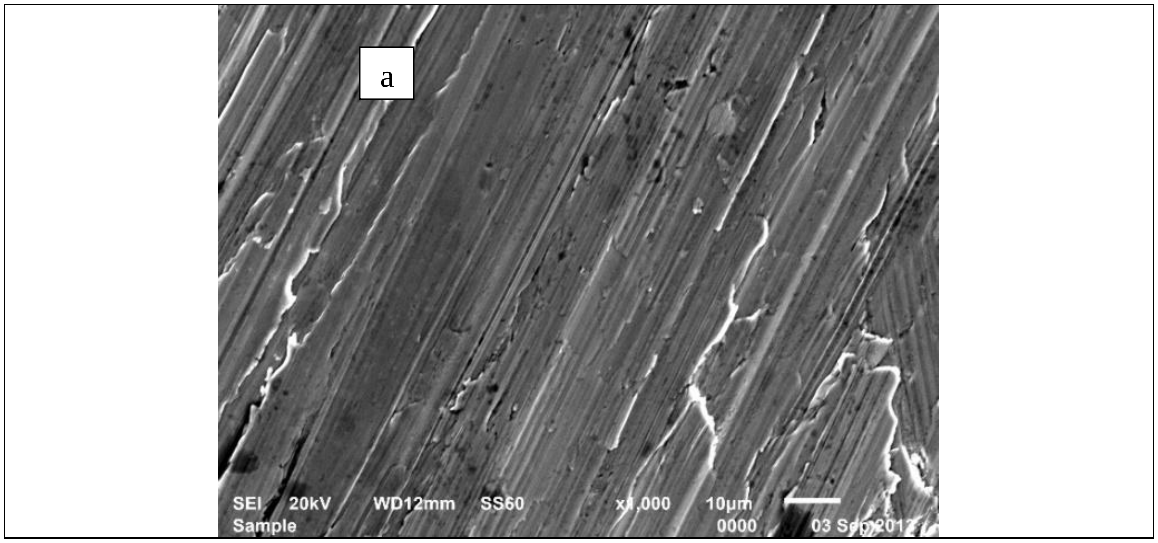

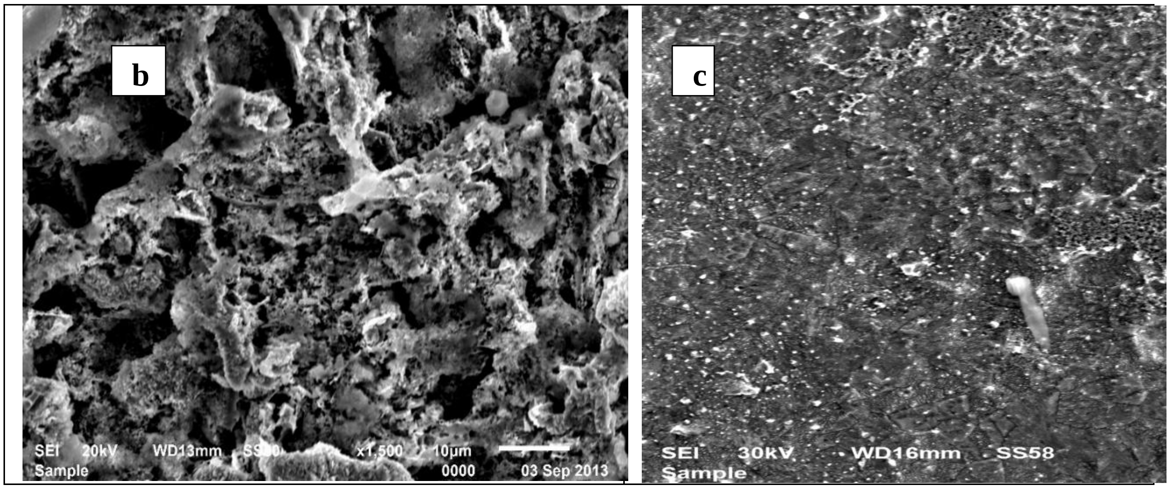

Figure 11: SEM micrographs of α-brass surface (a) before of immersion in 1 M HNO_3, (b) after 24 h of immersion in 1 M HNO_3, (c) after 24 h of immersion in 1 M HNO_3+ 5 ml\L of lemon oil at 25±1 °C.

Mechanism of Corrosion Inhibition

The inhibition mechanism involves the adsorption of the inhibitor on the metal surface immersed in aqueous HNO_3 solution. Four types of adsorption (37) may take place involving organic molecules at the metal–solution interface: 1)Electrostatic attraction between the charged molecules and the charged metal; 2) Interaction of unshared electron pairs in the molecule with the metal; 3) Interaction of π-electrons with the metal; 4) Combination of all the above. From the observations drawn from the different methods, corrosion inhibition of α-brass in 1M HNO_3 solutions by lemon oil as indicated from weight loss, potentiodynamic polarization and EIS techniques were found to depend on the concentration and the nature of the inhibition.

Conclusions

From the results of the study the following may be concluded:

1. Lemon oil is good corrosion inhibitor for α-brass in 1 M HNO_3 solution.
2. Reasonably good agreement was observed between the values obtained by the weight loss and electrochemical measurements were in good agreement.
3. Results obtained from potentiodynamic polarization indicated that lemon oil is mixed-type inhibitor.
4. Percentage inhibition efficiency of lemon oil was temperature dependent and its addition led to a decrease of the activation corrosion energy in all the studied acid media.
5. The thermodynamic parameters revealed that the inhibition of corrosion by lemon oil is due to the formation of a physical adsorbed film on the metal surface.
6. The adsorption of lemon oil onto α-brass surface follows the Temkin adsorption isotherm model.
7. The positive values of the free energy of adsorption and adsorption heat are indicating that the process was spontaneous and endothermic.

REFERENCES

(1) Li, S.L., Ma, H.Y., Lei, S.B., Yu, R., Chen, S.H., and Liu, D.X., Corrosion.**1998,** 54, 947.
(2) Stevanovic J., Skibina L. J., Stefanovic M., Despic A., Jovic V. D., J. Appl Electrochem.**1992,** 22, 172.
(3) Habib K., Amin A., Desalination.**1992,** 85, 275.
(4) Elrehim S. A., Assaf F. H., Elsayed A., Zaky A. M. Brit Corros J.**1995,** 30, 247.
(5) Morales J., Fernandez G. T., Esparza P., Gonzalez S., Sa R. C., Corros. Sci.**1995**, 37**,** 211.
(6) Badawy W. A., Al-Kharafi F. M., Corros Sci.**1999, 5**, 268.
(7) Rehan H. H., Al-Moubarak N. A., Al-Rafai H. A., Port Electrochim. Acta.**2003,** 21 (2), 99.
(8) Haquea M. M. and Faris Ismailb A., Adv Mater Res.**2008**, 7**,** 33-37.

(9) Mihit M., El Issami S., Bouklah M., Bazzi L., Hammouti B., Ait Addi E., Salghi R. and Kertit S., Appl Surf Sci.**2006,** 252 (6), 2389.
(10) Mu, G.N., Zhao, T.P., Liu, M., Gu, T., Corrosion .**1996**, 52, 853.
(11) Khaled K. F., Mater. Chem. Phys. **2008,**112, 290.
(12) Khaled K. F., J. Appl. Electrochem.**2009**, 39, 429.
(13)Bosch R. W., Hubrecht J., Bogaerts W. F., Syrett B. C., Corrosion.**2001**, 57, 60 .
(14) Abdel–Rehim S. S., Khaled K. F., Abd–Elshafi N. S., Electrochim. Acta. **2006**, 51, 3269.
(15) Banerjee G & Malhotra S N, Corrosion.**1992, 48**, 10.
(16) Hour T P & Holliday R D, J Appl Chem.**1953,** 3, 502.
(17) Riggs L O (Jr) & Hurd T J, Corrosion.**1967**, 23, 252.
(18) Schmid G M & Huang H J, Corros Sci.**1980**, 20, 1041.
(19) Bentiss F, Lebrini M & Lagrenee M, Corros Sci.**2005, 47**, 2915.
(20) Marsh J, Advanced Organic Chemistry, 3rd edn (Wieley Eastern, New Delhi), **1988.**
(21) Silverman D.C. and Carrico J. E., Corrosion.**1988,** 44, 280.
(22) Lorenz W. J.and Mansfeld F., Corros.Sci.**1981**, 21, 647.
(23) Macdonald D. D., Mckubre M. C., "Impedance measurements in Electrochemical systems," Modern Aspects of Electrochemistry, J.O'M. Bockris, B.E. Conway, R.E.White, Eds., Plenum Press, New York, New York, **1982**,14 61, .
(24) Mansfeld F.; Corrosion.**1981,** 36, 301.
(25) Gabrielli C.,"Identification of Electrochemical processes by Frequency Response Analysis,"Solarton Instrumentation Group, 1980.
(26) El Achouri M., Kertit S., Gouttaya H.M., Nciri B., Bensouda Y., Perez L., Infante M.R., Elkacemi K., Prog. Org. Coat.**2001**, 43, 267.
(27) Macdonald J.R., Johanson W.B., in: J.R. Macdonald (Ed.), Theory in Impedance Spectroscopy, John Wiley& Sons, New York, **1987**.
(28) Mertens S. F., Xhoffer C., Decooman B. C., E. Temmerman, Corrosion. **1997**, 53, 381.
(29) Trabanelli G., Montecelli C., Grassi V., Frignani A., J. Cem. Concr., Res.**2005**, 35, 1804 .
(30) Trowsdate A. J., Noble B., Haris S .J., Gibbins I.S. R., Thomson G. E., Wood G. C.,Corros. Sci.**1996**, 38, 177.
(31) Reis F. M., De Melo H.G. and Costa I., Electrochim. Acta. **2006,** 51, 17.
(32) Lagrenee M., Mernari B., Bouanis M., Traisnel M. & Bentiss F., Corros. Sci.**2002**, 44, 573.
(33) McCafferty E., Hackerman N., J. Electrochem. Soc.**1972,** 119, 146.
(34) Ma H., Chen S., Niu L., Zhao S., Li S., Li D., J. Appl. Electrochem.**2002**, 32, 65.
(35) Kus E., Mansfeld F., Corros. Sci.**2006**, 48, 965.
(36) Caigman G. A., Metcalf S. K., Holt E. M., J.Chem. Cryst.**2000,** 30, 415.
(37) Schweinsberg D. P., Graeme A., George, Nanayakkara A.K. and Steinert D.